Acta Cryst. (1996). B52, 140–144

The Location of *p*-Dichlorobenzene in a Single Crystal of Zeolite H-ZSM-5 at High Sorbate Loading

H. van Koningsveld, J. C. Jansen and H. van Bekkum

Laboratories of Applied Physics and Organic Chemistry and Catalysis, Delft University of Technology, Lorentzweg 1, 2628 CJ Delft, The Netherlands

(Received 8 October 1994; accepted 23 June 1995)

Abstract

The crystal structure of a high-loaded complex of H-ZSM-5 with eight molecules of *p*-dichlorobenzene per unit cell has been solved by single-crystal X-ray diffraction. The orthorhombic space group $P2_12_12_1$ with $a = 20.102\,(6)$, $b = 19.797\,(9)$, $c = 13.436\,(3)$ Å and $V = 5347\,(3)$ Å^3 has four $Si_{23.92}Al_{0.08}O_{48}.2C_6H_4Cl_2$ units per unit cell. $D_x = 2.164$ Mg m^{-3}, $\lambda(\text{Mo}\,K\alpha) = 0.71073$ Å and $\mu(\text{Mo}\,K\alpha) = 0.876$ mm^{-1}. The final $R(wR) = 0.046\,(0.039)$, $w = 1/\sigma^2(F)$, for 6090 observed reflections with $I > 1.0\sigma(I)$ measured at 293 K. The straight channel parallel to [010] is slightly corrugated. The elliptical cross sections have limiting apertures of 6.0 × 4.9 Å ($r_{\text{oxygen}} = 1.35$ Å). The sinusoidal channel parallel to [100] is elliptical with major and minor axes of 6.1 × 4.8 Å, respectively. One of the two independent *p*-dichlorobenzene molecule lies at the intersection of the straight and sinusoidal channels with its long molecular axis almost parallel to (100) and deviating ~ 8° from [010]. The second *p*-dichlorobenzene molecule is in the sinusoidal channel. Its long molecular axis deviates almost 7° from [100] and is practically parallel to (010). The structural aspects are in all details comparable to those in the high-loaded H-ZSM-5/*p*-xylene complex [van Koningsveld, Tuinstra, van Bekkum & Jansen (1989). *Acta Cryst.* B45, 423–431], except for the main interaction forces between the *p*-dichlorobenzene molecules at the channel intersection.

1. Introduction

Very recently the single-crystal structure analysis of a low-loaded complex of H-ZSM-5 with 2.6 molecules (mols) of *p*-dichlorobenzene (=3PDCB) per unit cell (u.c.) was completed (van Koningsveld, Jansen & de Man, 1996). The rotational orientation of the pdcb molecule at the intersection of channels is different from the orientation of the *p*-xylene molecule residing at the intersection in the high-loaded H-ZSM-5/8*p*-xylene complex (PARA; van Koningsveld *et al.*, 1989). The 10-ring in the straight channel of the (empty) orthorhombic H-ZSM-5 framework (=HTORTHO; van Koningsveld, 1990) has a clover-like pore opening. The minimal cross section of the absorbed molecule at the intersection of channels in 3PDCB and PARA corresponds to the two maximal limiting ports in the clover-like pore opening of HTORTHO, respectively. The same two orientations of the pdcb molecule at the intersection were calculated for silicalite-1 (the all silica H-ZSM-5) loaded with 4 pdcb mols/u.c. after full relaxation of the structure with fixed and variable unit-cell dimensions, respectively, using the software program *Discover*-3 from Biosym Technologies (1993). See also van Koningsveld *et al.* (1996).

A newly published paper (Mentzen & Sacerdote-Peronnet, 1993) describes the structure of high-loaded H-ZSM-5/8pdcb as determined from synchrotron X-ray powder data. The orientation of the pdcb molecule at the intersection of channels is similar to that of the corresponding *p*-xylene molecule in PARA. We succeeded in preparing a high-loaded single crystal of H-ZSM-5 with pdcb large enough to allow a single crystal study of the material.

2. Experimental

Calcined single crystals of H-ZSM-5, prepared according to a procedure described by van Koningsveld, Jansen & van Bekkum (1987), Si/Al ≈ 300, were placed in a 30 ml glass vessel and heated at 523 K for 5 h. The glass vessel was connected *via* a three-way valve to another 30 ml vessel containing excess pdcb. The valve was further connected to a vacuum system. After applying a vacuum to both vessels the connection between the two vessels was made. Subsequently the set-up was placed in a hot air oven. The temperature was then raised with 2 K min^{-1} to 373 K and kept constant for 60 min. Next the containers were cooled with 2 K min^{-1} to 333 K and maintained at that temperature for 60 min. This procedure was repeated several times. Finally, the crystals were cooled with 2 K min^{-1} to room temperature. The crystal selected for X-ray analysis measured 0.18, 0.12 and 0.25 mm in the *a*, *b* and *c* direction, respectively, and was mounted along the *c* axis.

Data were collected on a CAD-4 diffractometer using graphite-monochromated Mo *Kα* radiation ($\lambda = 0.71073$ Å). Full experimental details are given in Table 1. The unit-cell dimensions and orientation matrix were obtained from 25 carefully centred reflections with

Table 1. *Experimental details*

Crystal data	
Chemical formula	$C_{12}H_8Al_{0.08}Cl_4O_{48}Si_{23.92}$
Chemical formula weight	1736.09
Cell setting	Orthorhombic
Space group	$P2_12_12_1$
a (Å)	20.102 (6)
b (Å)	19.797 (9)
c (Å)	13.436 (3)
V (Å^3)	5347 (3)
Z	4
D_x (Mg m^{-3})	2.164
Radiation type	Mo $K\alpha$
Wavelength (Å)	0.71073
No. of reflections for cell parameters	25
θ range (°)	10–17
μ (mm^{-1})	0.876
Temperature (K)	293
Crystal form	Prismatic
Crystal size (mm)	0.25 × 0.18 × 0.12
Crystal colour	Light yellow
Data collection	
Diffractometer	CAD-4
Data collection method	ω–2θ
Absorption correction	None
No. of measured reflections	8471
No. of independent reflections	8471
No. of observed reflections	6090
Criterion for observed reflections	$I > 1.0\sigma(I)$
θ_{max} (°)	30
Range of h, k, l	$0 \rightarrow h \rightarrow 28$ $0 \rightarrow k \rightarrow 28$ $0 \rightarrow l \rightarrow 18$
No. of standard reflections	3
Frequency of standard reflections	Every 2 h
Intensity decay (%)	6.0
Refinement	
Refinement on	F
R	0.046
wR	0.039
S	2.27
No. of reflections used in refinement	6090
No. of parameters used	794
H-atom treatment	Fixed U riding on C
Weighting scheme	$w = 1/\sigma^2(F)$
$(\Delta/\sigma)_{max}$	0.11
$\Delta\rho_{max}$ (e Å^{-3})	0.97
$\Delta\rho_{min}$ (e Å^{-3})	−0.97
Extinction method	None
Source of atomic scattering factors	*Xtal*3.2 (Hall, Flack & Stewart, 1992)

$10 < \theta < 17°$. The intensity data were collected by ω–2θ scans, width $= (0.85 + 0.35\tan\theta)°$, requesting $\sigma_{count}(I)/I < 0.02$ in a scan or with a maximum recording time of 120 s. 8471 independent reflections were measured ($h = 0$–28, $k = 0$–28, $l = 0$–18, θ 0–30°), which gave 6091 reflections with $I > 1.0\sigma(I)$. Lorentz and polarization corrections were applied but no absorption corrections was made. The intial positions of the atoms were taken from the H-ZSM-5/8*p*-xylene structure (van Koningsveld *et al.*, 1989) with the methyl C atoms replaced by Cl atoms.*

Table 2. *Fractional atomic coordinates and equivalent isotropic displacement parameters (Å^2)*

$$U_{eq} = (1/3)\Sigma_i\Sigma_jU_{ij}a_i^*a_j^*\mathbf{a}_i.\mathbf{a}_j.$$

	x	y	z	U_{eq}
Si1	0.42470 (9)	0.06708 (9)	−0.2966 (1)	0.0107 (5)
Si2	0.31732 (9)	0.0319 (1)	−0.1479 (1)	0.0117 (6)
Si3	0.27933 (8)	0.0523 (1)	0.0734 (1)	0.0122 (5)
Si4	0.12277 (9)	0.0536 (1)	0.0653 (1)	0.0115 (5)
Si5	0.0745 (1)	0.0300 (1)	−0.1537 (1)	0.0121 (6)
Si6	0.1958 (1)	0.07036 (8)	−0.2810 (1)	0.0103 (4)
Si7	0.4263 (1)	−0.1693 (1)	−0.2946 (1)	0.0120 (5)
Si8	0.31731 (9)	−0.1274 (1)	−0.1495 (1)	0.0122 (6)
Si9	0.27446 (9)	−0.1737 (1)	0.0600 (1)	0.0107 (5)
Si10	0.11931 (9)	−0.1751 (1)	0.0574 (1)	0.0114 (5)
Si11	0.0736 (1)	−0.1285 (1)	−0.1534 (2)	0.0118 (6)
Si12	0.1953 (1)	−0.17235 (9)	−0.2803 (1)	0.0114 (5)
Si13	0.42448 (8)	0.4485 (1)	−0.3432 (1)	0.0118 (5)
Si14	0.3140 (1)	0.47058 (9)	−0.1906 (1)	0.0124 (5)
Si15	0.27878 (9)	0.4278 (1)	0.0216 (1)	0.0114 (5)
Si16	0.12146 (9)	0.4282 (1)	0.0224 (1)	0.0110 (5)
Si17	0.07348 (9)	0.4694 (1)	−0.1893 (1)	0.0112 (5)
Si18	0.19173 (9)	0.4498 (1)	−0.3383 (1)	0.0111 (4)
Si19	0.42685 (9)	0.6742 (1)	−0.3274 (1)	0.0116 (5)
Si20	0.3174 (1)	0.6274 (1)	−0.1829 (1)	0.0114 (5)
Si21	0.27647 (9)	0.6724 (1)	0.0243 (2)	0.0120 (5)
Si22	0.1217 (1)	0.6714 (1)	0.0223 (2)	0.0122 (6)
Si23	0.0730 (1)	0.6285 (1)	−0.1866 (2)	0.0122 (6)
Si24	0.1956 (1)	0.67338 (9)	−0.3167 (1)	0.0115 (4)
O1	0.3849 (2)	0.0620 (3)	−0.1933 (3)	0.020 (2)
O2	0.3170 (2)	0.0490 (3)	−0.0308 (3)	0.017 (1)
O3	0.2014 (3)	0.0527 (3)	0.0535 (3)	0.039 (2)
O4	0.0884 (3)	0.0502 (3)	−0.0406 (3)	0.031 (2)
O5	0.1263 (2)	0.0673 (3)	−0.2247 (3)	0.022 (2)
O6	0.2549 (2)	0.0658 (3)	−0.2024 (3)	0.021 (2)
O7	0.3851 (2)	−0.1566 (3)	−0.1952 (4)	0.024 (2)
O8	0.3139 (2)	−0.1436 (2)	−0.0336 (3)	0.018 (1)
O9	0.1969 (3)	−0.1573 (2)	0.0476 (3)	0.026 (1)
O10	0.0823 (3)	−0.1469 (3)	−0.0384 (4)	0.031 (2)
O11	0.1276 (3)	−0.1655 (3)	−0.2202 (4)	0.030 (2)
O12	0.2564 (3)	−0.1620 (3)	−0.2062 (4)	0.029 (2)
O13	0.3138 (3)	−0.0476 (3)	−0.1675 (3)	0.029 (2)
O14	0.0819 (3)	−0.0495 (3)	−0.1677 (4)	0.037 (2)
O15	0.4119 (3)	0.1391 (2)	−0.3458 (3)	0.020 (2)
O16	0.3997 (3)	0.0101 (3)	−0.3709 (4)	0.032 (2)
O17	0.3994 (3)	−0.1209 (3)	−0.3811 (4)	0.031 (2)
O18	0.1984 (3)	0.1404 (2)	−0.3400 (3)	0.017 (1)
O19	0.2017 (3)	0.0104 (2)	−0.3604 (3)	0.030 (2)
O20	0.1996 (3)	−0.1198 (2)	−0.3704 (3)	0.029 (2)
O21	0.0014 (2)	0.0514 (3)	−0.1852 (3)	0.024 (2)
O22	0.0027 (3)	−0.1540 (3)	−0.1896 (4)	0.028 (2)
O23	0.4186 (2)	−0.2452 (3)	−0.3313 (4)	0.025 (2)
O24	0.1981 (3)	−0.2470 (2)	−0.3269 (3)	0.023 (1)
O25	0.2860 (2)	−0.2533 (2)	0.0669 (3)	0.020 (1)
O26	0.1097 (2)	−0.2544 (3)	0.0672 (4)	0.024 (2)
O27	0.3825 (2)	0.4520 (4)	−0.2428 (3)	0.032 (2)
O28	0.3064 (3)	0.4280 (2)	−0.0897 (3)	0.019 (1)
O29	0.1998 (3)	0.4352 (2)	0.0204 (3)	0.035 (2)
O30	0.0923 (3)	0.4324 (2)	−0.0871 (3)	0.025 (2)
O31	0.1255 (2)	0.4508 (3)	−0.2746 (3)	0.026 (2)
O32	0.2546 (2)	0.4548 (3)	−0.2661 (3)	0.027 (2)
O33	0.3860 (3)	0.6446 (3)	−0.2361 (4)	0.026 (2)
O34	0.3150 (3)	0.6668 (2)	−0.0798 (3)	0.024 (2)
O35	0.1987 (3)	0.6571 (2)	0.0074 (4)	0.034 (2)
O36	0.0857 (3)	0.6650 (3)	−0.0822 (4)	0.035 (2)
O37	0.1282 (3)	0.6494 (3)	−0.2660 (4)	0.031 (2)
O38	0.2572 (3)	0.6488 (3)	−0.2518 (4)	0.034 (2)
O39	0.3125 (3)	0.5481 (3)	−0.1609 (3)	0.034 (2)
O40	0.0733 (3)	0.5490 (3)	−0.1708 (3)	0.031 (2)
O41	0.4073 (3)	0.3813 (3)	−0.4002 (5)	0.042 (2)
O42	0.4089 (3)	0.5120 (3)	−0.4118 (4)	0.031 (2)
O43	0.3989 (3)	0.6429 (2)	−0.4296 (4)	0.020 (2)
O44	0.1941 (3)	0.3806 (2)	−0.3983 (3)	0.023 (1)
O45	0.1909 (3)	0.5111 (2)	−0.4156 (3)	0.022 (1)
O46	0.2001 (3)	0.6414 (2)	−0.4268 (3)	0.022 (1)
O47	0.0023 (2)	0.4432 (3)	−0.2258 (3)	0.023 (2)

---

* For a direct comparison with other MFI frameworks, the origin in $P2_12_12_1$ is shifted to $(0, 0, \frac{1}{4})$. The symmetry operations become: x, y, z; $x + \frac{1}{2}, \frac{1}{2} - y, \frac{1}{2} - z$; $-x, y + \frac{1}{2}, -z$; $\frac{1}{2} - x, -y, \frac{1}{2} + z$.

Table 2 (*cont.*)

	x	y	z	U_{eq}
O48	0.0026 (3)	0.6527 (3)	−0.2286 (4)	0.024 (2)
Cl1	0.0626 (1)	0.2404 (2)	−0.1083 (2)	0.094 (1)
Cl2	0.3685 (1)	0.2599 (2)	−0.1557 (2)	0.089 (1)
C1	0.1480 (5)	0.2480 (6)	−0.1193 (8)	0.062 (4)
C2	0.1736 (5)	0.2841 (4)	−0.1956 (6)	0.047 (3)
C3	0.2433 (5)	0.2875 (5)	−0.2080 (6)	0.049 (3)
C4	0.2815 (5)	0.2556 (5)	−0.1377 (7)	0.059 (4)
C5	0.2552 (7)	0.2203 (5)	−0.0626 (6)	0.068 (4)
C6	0.1899 (7)	0.2171 (5)	−0.0478 (6)	0.068 (4)
Cl10	0.5158 (3)	0.3988 (3)	−0.0552 (3)	0.158 (3)
Cl20	0.5095 (3)	0.0889 (3)	0.0102 (4)	0.184 (3)
C10	0.5142 (7)	0.3077 (9)	−0.042 (1)	0.114 (8)
C20	0.4859 (7)	0.286 (1)	0.0420 (9)	0..114 (8)
C30	0.4815 (7)	0.214 (1)	0.0665 (8)	0.127 (9)
C40	0.5098 (6)	0.1735 (8)	−0.009 (1)	0.092 (6)
C50	0.5358 (8)	0.201 (1)	−0.099 (1)	0.126 (9)
C60	0.5365 (8)	0.270 (1)	−0.108 (1)	0.15 (1)

All T atoms (Si,Al) were treated as zero-valent Si. The population of the pdcb molecules refine to 1.013 (3) and 0.993 (3) for the molecules at the intersection of channels and in the sinusoidal channel, respectively. The population parameters of the pdcb molecules were reset to 1.0, corresponding to 8 pdcb mols/u.c. H atoms were included at calculated positions (C—H = 1.0 Å) and refined with fixed isotropic U values riding on the parent C atoms. Anisotropic refinement of the framework atoms on F, without any constraints on the adsorbed pdcb molecules, converged to $R = 0.046$, $wR = 0.039$ [$w^{-1} = \sigma^2(F)$] and $S = 2.27$ for 6090 observed reflections (one low-order reflection excluded) and 794 variables. The average and maximum shift/e.s.d. were 0.003 and 0.11 [U_{23} of C(10)], respectively. The final ΔF synthesis has $|\rho| < 0.97\,e\,Å^{-3}$ with peaks in close vicinity of the framework atoms. The synthesis is featureless elsewhere. All calculations were performed on a SUN-IPX workstation using the programs of the *Xtal*3.2 system (Hall, Flack & Stewart, 1992). Final positional and equivalent isotropic displacement parameters of the high-loaded H-ZSM-5/8pdcb (=8PDCB) are given in Table 2. After storage for several months at ambient the unit-cell dimensions and symmetry were redetermined at 295 K. No significant changes were observed. This proves the stability of the complex at atmospheric pressure and room temperature.

Table 3. *Comparison of the framework geometry in H-ZSM-5/8pdcb (=8PDCB) and H-ZSM-5/8p-xylene (=PARA)*

	8PDCB	PARA
O—Si—O range (°)	106.9–112.1 (4)	107.5–112.0 (2)
Av. O—Si—O/SiO$_4$	109.47	109.47
Si—O range (Å)	1.573–1.612 (5)	1.574–1.611 (4)
Range of av. Si(O)$_4$	1.585–1.603	1.588–1.604
Av. Si—O	1.594	1.597
Si—O—Si range (°)	138.8–176.9 (5)	138.3–172.3 (3)
Range of av. Si(OSi)$_4$	149.1–164.1	148.5–162.3
Av. Si—O—Si	155.1	154.7

Table 4. *Pore openings ('diagonal' O· · ·O distances, Å) in the double 10-rings in 8PDCB and PARA together with the results obtained by Mentzen & Sacerdote-Peronnet (1993) from synchrotron powder data on H-ZSM-5/8pdcb (XPD)*

Maximal and minimal pore dimensions, corresponding to the same diagonal distances in 10-rings, are underlined.* The O-atom numbering, modulus 26, corresponds to that in Fig. 2.

	8PDCB	PARA	XPD
Straight channel sections			
O(1)—O(33)	$\underline{7.560}$ (7)	$\underline{7.503}$ (5)	$\underline{7.72}$ (4)
O(2)—O(34)	7.898 (7)	7.968	7.96
O(20)—O(44)	8.504 (9)	8.489	8.38
O(11)—O(31)	$\underline{8.790}$ (8)	$\underline{8.882}$	$\underline{8.66}$
O(22)—O(47)	8.087 (7)	8.071	8.08
1/s†	1.162	1.184	1.122
O(7)—O(27)	$\underline{7.817}$ (7)	$\underline{7.774}$ (5)	$\underline{7.92}$ (4)
O(8)—O(28)	7.938 (7)	7.949	8.06
O(18)—O(46)	8.602 (80	8.615	8.46
O(5)—O(37)	$\underline{8.697}$ (7)	$\underline{8.755}$	$\underline{8.65}$
O(21)—O(48)	8.127 (7)	8.099	8.14
1/s†	1.113	1.126	1.092
Sinusoidal channel sections			
O(1)—O(8)	7.545 (8)	7.578 (5)	7.64 (4)
O(2)—O(27)	8.574 (9)	8.606	8.70
O(20)—O(41)	$\underline{9.060}$ (8)	$\underline{9.071}$	$\underline{8.90}$
O(24)—O(26)	8.333 (7)	8.302	8.25
O(15)—O(46)	$\underline{7.461}$ (7)	$\underline{7.456}$	$\underline{7.55}$
1/s†	1.214	1.217	1.179
O(5)—O(30)	7.491 (8)	7.447 (5)	7.62 (4)
O(4)—O(31)	8.565 (9)	8.533	8.45
O(17)—O(44)	$\underline{8.846}$ (7)	$\underline{8.846}$	$\underline{8.78}$
O(23)—O(25)	8.515 (7)	8.591	8.62
O(18)—O(43)	$\underline{7.257}$ (6)	$\underline{7.283}$	$\underline{7.32}$
1/s†	1.219	1.215	1.199

* One of the possible ways to calculate the 'diagonal' O· · ·O distances in 8PDCB is deposited as supplementary material to Table 4. † 1/s: ratio of longest and shortest O· · ·O distance.

3. Discussion

3.1. *Geometry of the zeolite framework*

Distances and angles are summarized in Table 3,* together with the corresponding values in PARA. The range of O—Si—O angles and Si—O distances is essentially equal in both structures. Subtle differences between the frameworks become apparent from the differences in the range and the individual values of Si—O—Si angles and in the pore sizes. A comparison between the pore openings in the double 10-rings in the straight and sinusoidal channels in 8PDCB and PARA, described by the 'diagonal' O· · ·O distances, is given in Table 4. The results obtained by Mentzen & Sacerdote-Peronnet (1993) from synchrotron powder diffraction data on H-ZSM-5/8pdcb are added to Table 4. The pore dimensions obtained in our analysis deviate much less from those in PARA than the results reported by

---

* Lists of structure factors, anisotropic thermal parameters and complete geometry have been deposited with the IUCr (Reference: HU0427). Copies may be obtained through The Managing Editor, International Union of Crystallography, 5 Abbey Square, Chester CH1 2HU, England.

Table 5. *Comparison of bond lengths (Å) and angles (°) in pdcb molecules at the intersection of channels (pdcb1) and in the sinusoidal channel (pdcb2) with the corresponding values in pdcb single crystals at 100 K (Wheeler & Colson, 1975; W&C)*

	pdcb1	pdcb2	*W&C**
C(1)—C(2)	1.33 (2)	1.35 (1)	1.389 (5)
C(2)—C(3)	1.48 (3)	1.41 (1)	1.394 (5)
C(3)—C(4)	1.41 (2)	1.37 (1)	1.390 (4)
C(4)—C(5)	1.42 (2)	1.34 (1)	1.389 (5)
C(5)—C(6)	1.36 (3)	1.33 (1)	1.394 (5)
C(6)—C(1)	1.26 (3)	1.42 (1)	1.390 (4)
mean	1.38	1.37	1.391
C(1)—Cl(1)	1.81 (2)	1.73 (1)	1.749 (3)
C(4)—Cl(2)	1.70 (2)	1.77 (1)	1.749 (3)
mean	1.76	1.75	1.749
C(1)—C(2)—C(3)	122 (2)	119.5 (8)	118.8 (2)
C(2)—C(3)—C(4)	111 (1)	116.9 (8)	119.1 (3)
C(4)—C(5)—C(6)	118 (2)	122 (1)	118.8 (2)
C(5)—C(6)—C(1)	122 (2)	117.7 (9)	119.1 (3)
mean	118	119.1	118.9
C(2)—C(1)—C(6)	124 (2)	121.1 (9)	122.1 (3)
C(3)—C(4)—C(5)	123 (2)	123 (1)	122.1 (3)
mean	124	121.8	122.1
C(2)—C(1)—Cl(1)	114 (1)	119.2 (8)	119.1 (2)
C(6)—C(1)—Cl(1)	121 (2)	119.7 (8)	118.8 (3)
C(3)—C(4)—Cl(2)	116 (1)	115.9 (7)	118.8 (3)
C(5)—C(4)—Cl(2)	121 (1)	121.4 (8)	119.1 (2)
mean	118	119.1	118.9

* Pdcb has a centre of symmetry.

Mentzen & Sacerdote-Peronnet (1993). The pores, as determined from their powder data, are in general less elliptical (*cf.* the $1/s$ values listed in Table 4).

3.2. *Geometry and packing of p-dichlorobenzene*

Distances and angles in pdcb, after anisotropic refinement without any constraints on the atoms, are given in Table 5. Molecule pdcb1 is located at the intersection of the straight and the sinusoidal channel and pdcb2 lies in the sinusoidal channel (Fig. 1). The Cl—Cl axis in pdcb1 deviates ~8° from [010] and is nearly parallel to (100). The angle of the normal on the benzene ring plane and positive *a* axis is −26.2°. This orientation differs by (47.1 + 26.2)° from the rotational orientation of pdcb at the intersection of channels in the low-loaded H-ZSM-5/2.6 pdcb complex (Fig. 2; van Koningsveld *et al.*, 1996) and agrees with one of the maximal pore directions in the clover-like pore windows in the straight channel of HTORT. The long molecular Cl—Cl axis in pdcb2 deviates almost 7° from [100] and is practically parallel to (010). The minimal cross section of the pdcb molecules fills the maximal limiting ports in both channels. The mean bond distances and bond angles in both pdcb molecules (Table 5) are in fairly good agreement with the corresponding values determined by X-ray analysis of pdcb single crystals (Wheeler & Colson, 1975). The Cl—Cl contact between Cl atoms in neighbouring pdcb1 molecules in the straight channel is 3.846 (8) Å, in reasonable agreement with the inter-

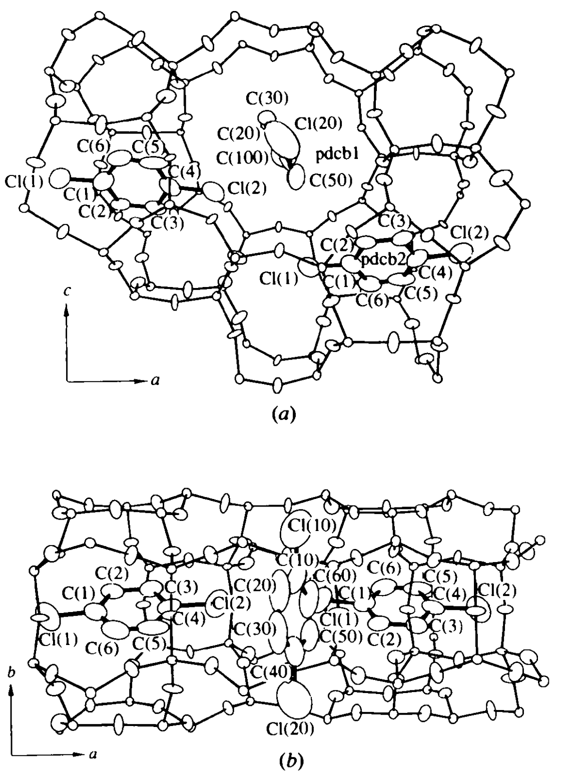

Fig. 1. *ORTEP* drawings (Johnson, 1965) of 8PDCB. (*a*) View down the straight channel axis. Pdcb1 at intersection of channels; pdcb2 in the sinusoidal channel. (*b*) View approximately along [001]. H atoms are omitted for clarity. The ellipsoids are drawn to enclose 50% probability.

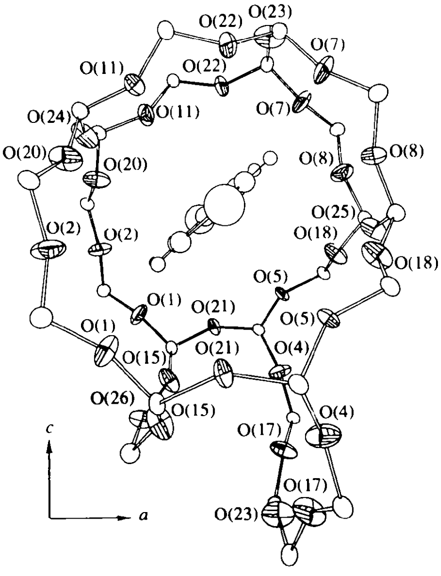

Fig. 2. View down the straight channel axis in the low-loaded H-ZSM-5/2.6 pdcb complex (van Koningsveld *et al.*, 1996), showing the orientation of pdcb at the intersection of channels and the O atom numbering.

Table 6. *p-Dichlorobenzene-to-framework contacts (<3.70 Å) and pdcb1-to-pdcb2 distances (<4.00 Å)*

pdcb1-framework			
Cl(10)—O(21$^{\mathrm{i}}$)	3.636 (7)	C(30)—O(22$^{\mathrm{iv}}$)	3.50 (1)
C(20)—O(7$^{\mathrm{ii}}$)	3.50 (2)	C(50)—O(44$^{\mathrm{i}}$)	3.57 (2)
C(20)—O(37$^{\mathrm{iii}}$)	3.68 (2)	C(60)—O(25$^{\mathrm{ii}}$)	3.64 (2)
C(20)—O(48$^{\mathrm{iii}}$)	3.32 (2)		
pdcb2-framework			
Cl(1)—O(26$^{\mathrm{v}}$)	3.510 (5)	C(3)—O(32)	3.41 (1)
Cl(1)—O(43$^{\mathrm{iii}}$)	3.422 (6)	C(3)—O(44)	3.30 (1)
Cl(2)—O(15)	3.607 (6)	C(4)—O(28)	3.51 (1)
Cl(2)—O(28)	3.662 (6)	C(4)—O(46$^{\mathrm{iii}}$)	3.51 (1)
C(1)—O(43$^{\mathrm{iii}}$)	3.47 (1)	C(5)—O(2)	3.64 (1)
C(2)—O(18)	3.480 (9)	C(5)—O(6)	3.59 (1)
C(2)—O(25$^{\mathrm{vi}}$)	3.349 (9)	C(5)—O(20$^{\mathrm{iv}}$)	3.38 (1)
C(2)—O(30)	3.66 (1)	C(5)—O(24$^{\mathrm{iv}}$)	3.35 (1)
C(2)—O(31)	3.60 (1)	C(5)—O(46$^{\mathrm{iii}}$)	3.41 (1)
C(2)—O(44)	3.353 (9)	C(6)—O(3)	3.53 (1)
C(3)—O(18)	3.53 (1)	C(6)—O(17$^{\mathrm{iv}}$)	3.44 (1)
C(3)—O(25$^{\mathrm{vi}}$)	3.154 (9)	C(6)—O(23$^{\mathrm{iv}}$)	3.68 (1)
C(3)—O(28)	3.44 (1)	C(6)—O(43$^{\mathrm{iii}}$)	3.66 (1)
pdcb2-to-pdcb1			
Cl(2)—C(10)	3.44 (2)	Cl(2)—C(60)	3.44 (2)
Cl(2)—C(20)	3.59 (1)	Cl(1)—C(60$^{\mathrm{vii}}$)	3.85 (2)
Cl(2)—C(30)	3.86 (1)	C(2)—C(50$^{\mathrm{vii}}$)	3.93 (2)
Cl(2)—C(40)	3.86 (1)	C(2)—C(60$^{\mathrm{vii}}$)	3.96 (2)
Cl(2)—C(50)	3.64 (2)		

Symmetry codes: (i) $\frac{1}{2}+x, \frac{1}{2}-y, -\frac{1}{2}-z$; (ii) $-x+1, \frac{1}{2}+y, -z$; (iii) $\frac{1}{2}-x, -y+1, \frac{1}{2}+z$; (iv) $\frac{1}{2}-x, -y, \frac{1}{2}+z$; (v) $-x, \frac{1}{2}+y, -z$; (vi) $\frac{1}{2}-x, -y, -\frac{1}{2}-z$; (vii) $-\frac{1}{2}+x, \frac{1}{2}-y, -\frac{1}{2}-z$.

Table 7. *Geometry of short C—O contacts (C—O < 3.70, C—H = 1.0 Å) with H· · ·O smaller than 2.8 Å*

Contact	C· · ·O (Å)	H· · ·O (Å)	C—H· · ·O (°)
C(2)—H(2)· · ·O(44)	3.353 (9)	2.731 (5)	120.7 (5)
C(3)—H(3)· · ·O(25$^{\mathrm{i}}$)	3.154 (9)	2.726 (5)	106.2 (5)
C(3)—H(3)· · ·O(44)	3.30 (1)	2.644 (5)	123.5 (6)
C(5)—H(5)· · ·O(20$^{\mathrm{ii}}$)	3.38 (1)	2.486 (5)	149.3 (7)
C(5)—H(5)· · ·O(24$^{\mathrm{ii}}$)	3.35 (1)	2.759 (4)	117.9 (5)
C(6)—H(6)· · ·O(17$^{\mathrm{ii}}$)	3.44 (1)	2.479 (6)	161.9 (7)
C(20)—H(20)· · ·O(37$^{\mathrm{iii}}$)	3.68 (2)	2.792 (6)	148 (1)
C(20)—H(20)· · ·O(48$^{\mathrm{iii}}$)	3.32 (2)	2.575 (5)	131.1 (8)
C(30)—H(30)· · ·O(22$^{\mathrm{ii}}$)	3.50 (1)	2.676 (3)	139.6 (8)
C(30)—H(30)· · ·O(11$^{\mathrm{ii}}$)	3.73 (1)	2.763 (6)	162.9 (9)

Symmetry codes: (i) $\frac{1}{2}-x, -y, -\frac{1}{2}-z$; (ii) $\frac{1}{2}-x, -y, \frac{1}{2}+z$; (iii) $\frac{1}{2}-x, -y+1, \frac{1}{2}+z$.

molecular Cl—Cl contacts in a pure γ-*p*-dichlorobenzene crystal [3.789 (2) and 3.800 (2) Å; Wheeler & Colson (1975)], although the packing in the latter crystal is quite different. In the sinusoidal channel, the shortest Cl—Cl distance between Cl atoms in adjacent pdcb2 molecules is 5.029 (4) Å, indicating that the packing forces between pdcb2 molecules are negligible.

The shortest intermolecular Cl—Cl contact between pdcb1 and pdcb2 is 4.260 (6) Å [Cl(2)—Cl(10)]. The next shortest Cl—Cl distance is 4.946 (7) Å between Cl(2) and Cl(20). The Cl—Cl distances between Cl(1) and the Cl atoms in pdcb1 are larger than 5.3 Å.

Short pdcb-to-framework distances are summarized in Table 6, together with C—C and C—Cl contacts between pdcb1 and pdcb2 molecules. Table 7 summarizes the geometry of some short C—O contacts which might exhibit (weak) H· · ·O interactions. Pdcb2 in the sinusoidal channel is more tightly packed than pdcb1 at the intersection (see Tables 6 and 7).

The closer packing of pdcb2 is also apparent from the smaller e.s.d.'s in the observed bond distances and angles and from the lower displacement parameters (Tables 5 and 2).

The packing arrangement of pdcb1 and pdcb2 is not significantly different from that observed for the two independent *p*-xylene molecules in PARA. The interaction forces between pdcb1 and pdcb2, however, are quite different. In PARA, the molecules are trapped at the channel intersections by establishing contacts between a methyl (H) atom in the one *p*-xylene molecule to the aromatic ring atoms in the adjacent *p*-xylene molecule. This arrangement is analogous to that in pure *p*-xylene single crystals (van Koningsveld, van den Berg, Jansen & de Goede, 1986) and apparently represent rather firm interactions.* In 8PDCB, however, these methyl(H)· · ·aromatic ring interactions are replaced by Cl· · ·C interactions (see Table 6), which are substantially weaker. The importance of the interactions of the guest molecules at the intersection in stabilizing the guest structure within the zeolite host framework might therefore need reconsideration. The C· · ·O contacts listed in Table 7 are the same in both 8PDCB and PARA structures and might be, besides the flexible response of the channel pores, the main stabilizing forces for the actually observed packing arrangement.

---

* Upon desorption of *p*-xylene form PARA, the interaction forces between the methyl (H) atom and the aromatic ring atoms have to be surmounted and hysteresis occurs.

References

Biosym Technologies (1993). *Biosym Catalysis and Sorption Software*. Version 3. Biosym Technologies, San Diego.

Hall, S. R., Flack, H. D. & Stewart, J. M. (1992). Editors. *Xtal3.2 Reference Manual*. Universities of Western Australia, Australia, Geneva, Switzerland, and Maryland, USA.

Johnson, C. K. (1965). *ORTEP*. Report ORNL-3794, revised, June 1970. Oak Ridge National Laboratory, Tennessee, USA.

Koningsveld, H. van (1990). *Acta Cryst.* **B46**, 731–735.

Koningsveld, H. van, van den Berg, A. J., Jansen, J. C. & de Goede, R. (1986). *Acta Cryst.* **B42**, 491–497.

Koningsveld, H. van, Jansen, J. C. & van Bekkum, H. (1987). *Zeolites*, **7**, 564–568.

Koningsveld, H. van, Jansen, J. C. & de Man, A. J. M. (1996). *Acta Cryst.* **B52**, 131–139.

Koningsveld, H. van, Tuinstra, F., van Bekkum, H. & Jansen, J. C. (1989). *Acta Cryst.* **B45**, 423–431.

Mentzen, B. F. & Sacerdote-Peronnet, M. (1993). *Mat. Res. Bull.* **28**, 1161–1168.

Wheeler, G. L. & Colson, S. D. (1975). *Acta Cryst.* **B31**, 911–913.